UNIVERSITÁ DEGLI STUDI DI MILANO BICOCCA

Dipartimento di Fisica

Corso di Laurea Triennale

Qubit reduction techniques for bosonic systems

Supervisor:

Prof. Andrea Giachero

Co-supervisor:

Pietro Campana

Candidate:

Martina Piccamiglio

ACADEMIC YEAR 2022/2023

Abstract

Quantum computing emerged and evolved with the promise of surpassing the constraints of classical computation. Simulating quantum systems on classical devices poses significant difficulties. Take, for example, a system of electrons comprising N orbitals. In such a system, there exist 2^N possible configurations. As N grows, the required memory scales exponentially, quickly surpassing the memory capacities even of the most powerful supercomputers.

In 1981, Richard Feynman proposed that, given the non-classical nature of the natural world, it might be more efficient to employ hardware based on quantum phenomena for simulating physical systems. Since then, the field has garnered substantial interest and investments. The early 21st century witnessed an intense competition among researchers and tech companies, to build quantum computers. This period marked significant progress in the advancement of various quantum computing technologies. The current state of quantum computing is commonly denoted as the Noisy Intermediate-Scale Quantum (NISQ) era.

Today quantum computers are enabling interesting experimentation and research, but quantum advantage, which occurs when a quantum algorithm demonstrates a considerable speedup compared to the best possible algorithm on a classical computer, has only been achieved in very limited instances. NISQ devices have not yet succeeded in providing solutions to problems of real scientific significance. At the moment, current quantum computers face several constraints: quantum systems are sensitive to interactions with the environment, which lead to noise and loss of their quantum properties, a phenomenon known as decoherence. Building quantum computers able to manipulate hundreds or thousands of qubits while maintaining high levels of coherence poses a significant challenge. Therefore, in the present day, optimizing resources to execute quantum algorithms is crucial: the number of required qubits is a key factor in computational efficiency, since controlling quantum errors and processing information becomes progressively more difficult as the number of qubits involved grows.

Several approaches have been developed in order to reduce the qubits requirements.

This thesis introduces one such reduction method known as Qubit Tapering. Moreover, while Qubit Tapering is commonly employed in fermionic problems, this work also aims to investigate its application to interacting bosons systems.

The first chapter introduces some basic concepts of quantum computing, including the definition of qubits and quantum logic gates. The stabilizer formalism is then presented. While originally developed in the context of quantum error correction, the stabilizer formalism can also be used to construct specific system symmetries that enable the removal of certain qubits from the simulation. Finally, the Tapering method is discussed, along with an example of the physical interpretation of the symmetries found when applying Qubit Tapering to quantum chemistry problems.

The second chapter presents the chosen physical system for applying and studying Qubit Tapering. Firstly, the formalism known as Occupation Number Representation (or Second Quantization) is presented, providing a framework for describing quantum many-body systems composed of identical particles. Following this, the chapter outlines the Bose-Hubbard model, a widely studied lattice-based system of bosons. The discussion extends to quantum phase transitions, transformations of certain physical systems resulting in a radical alteration of their properties. In the Bose-Hubbard model, a quantum phase transition occurs due to the competition between the kinetic and interaction terms of the

Hamiltonian. The chapter concludes by introducing qubit encodings for bosonic systems, that enable a transition from a representation based on Fock states to the one implemented on a quantum computer.

The third chapter focuses on the implementation of the Bose-Hubbard Hamiltonian in the qubit Hilbert space, expressed as a sum of Pauli strings. A class named BoseHubbardHamiltonian is implemented in Python, on whose instances the Tapering procedure is applied. The lattice construction is based on the use of Qiskit Nature's Lattice classes, a framework designed to address problems in quantum mechanics related to natural sciences using quantum algorithms. The reduction of qubit requirements for the system is accomplished using the Python package Symmer.

The Tapering procedure is applied to different types of lattices, including linear, closed, with or without geometric symmetries, and finally, to three-dimensional lattices. In all these cases, a single symmetry of the same type is obtained, leading to the removal of one qubit. The physical meaning of this symmetry is interpreted as the parity of the number of bosons constituting the system, which remains constant. The applicability of tapering to other symmetries of the system is then investigated. Actually, the symmetries allowing Tapering have specific characteristics, and mere commutation with the system's Hamiltonian is not sufficient.

Finally, according to the theory underlying Tapering, one expects the eigenvalues of the reduced Hamiltonian to coincide with those of the initial Hamiltonian. This expectation is confirmed by numerical comparisons.

Contents

Chapter 1

A quantum computer is a device capable of harnessing the properties of quantum physics to perform calculations and process data more efficiently than a classical computer. As classical computers describe data using bits and operate on them with logic circuits made of logic gates, quantum computers, in a similar fashion, use quantum bits, known as *qubits*, and gates that allow to manipulate their state. From a physical standpoint, qubits are quantum states with two levels. Their quantum nature allows them to exist in a superposition of states, enabling a more complex representation of information compared to classical bits. [16] [31]

However, when a circuit is executed on an actual quantum computer, noise is introduced: at each step of the circuit, if the expected state of the system is $|\psi\rangle$, the measured state may instead be $|\tilde{\psi}\rangle$. Such discrepancies can arise from unwanted interactions between qubits or the system's interactions with the environment. Quantum states are inherently fragile, making the achievement of quantum advantage difficult. Because of this, some of the major efforts in quantum computing focus on building a model of quantum errors and develop a theory for error detection and correction.

In this situation, the *Stabilizer formalism* is extremely useful in managing quantum errors. [21]. Stabilizers were first introduced in the context of quantum error correction by Daniel Gottesman, in his PhD thesis, in 1997 [11].

Moreover, the Stabilizer formalism can be exploited to reduce the number of qubits describing a system in a quantum algorithm. Indeed, the more qubits are required to describe a physical system, the higher the likelihood of errors and the complexity involved in processing information and executing operations. It is therefore crucial to optimize the utilization of computational resources.

In a quantum system governed by a Hamiltonian H, stabilizers can represent specific symmetries. These symmetries are subsequently utilized to optimize computational resources.[26] This method, known as *Qubit Tapering*, has been primarily applied to fermionic systems and in quantum chemistry, an area of research focused on studying properties of molecules using quantum mechanics. [2] Nevertheless, it is very useful to delve into its utilization in the case of bosonic systems.

1.1 Quantum computing

1.1.1 Quantum bits

In classical computation, a bit is the fundamental unit of information: it is a state that can take on the values 0 and 1. A qubit, on the other hand, is a two-level quantum system

characterized by two states $|0\rangle$ and $|1\rangle$. Due to its quantum mechanical nature, a qubit can exist in any state of the form:

$$|\psi\rangle = \alpha |0\rangle + \beta |1\rangle \tag{1.1}$$

The parameters α and β are complex numbers. They define the quantum state of a qubit, which can be seen as a vector in a two-dimensional Hilbert space, where

$$|0\rangle = \begin{pmatrix} 1 \\ 0 \end{pmatrix} \quad ; \quad |1\rangle = \begin{pmatrix} 0 \\ 1 \end{pmatrix} \tag{1.2}$$

and then

$$|\psi\rangle = \begin{pmatrix} \alpha \\ \beta \end{pmatrix} \tag{1.3}$$

When a qubit is measured, the result obtained can be either $|0\rangle$ with probability $|\alpha|^2$ or $|1\rangle$ with probability $|\beta|^2$. Since probabilities must sum up to one, $|\alpha|^2 + |\beta|^2 = 1$. The special states $|0\rangle$ and $|1\rangle$ form an orthonormal basis for the vector space. A useful representation of qubits is the following. Since $|\alpha|^2 + |\beta|^2 = 1$, a quantum bit can be written as

$$|\psi\rangle = cos\frac{\theta}{2} |0\rangle + e^{i\phi} sin\frac{\theta}{2} |1\rangle \tag{1.4}$$

The parameters θ and ϕ identify a point on the unitary three-dimensional sphere, which is called the *Bloch Sphere*. There are infinite points on the sphere, in the same way there are infinite combinations of α and β in the definition of a qubit.
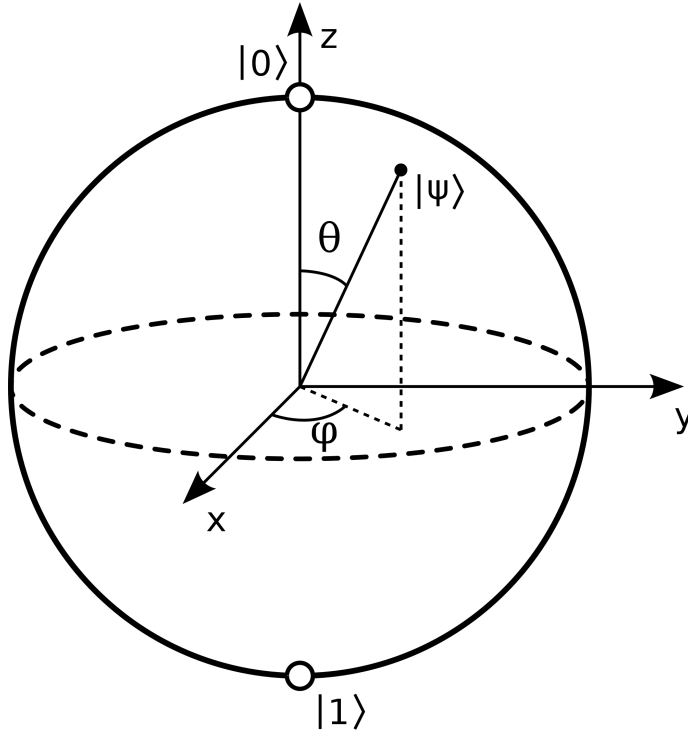

Figure 1.1: Bloch sphere representation of a qubit.

Physically, a qubit can be obtained from any quantum system with two distinct states. Some examples of physical qubits include [31]:

- Photons: a photon's polarization can be vertical or horizontal, or a superposition of both, and it can be used as a qubit;

- Trapped ions: ions can be trapped using electric fields, and once this is done, two energy levels of an ion can be used as a qubit;

- Cold atoms: neutral atoms can be trapped at low temperatures, and once trapped, two energy levels of an atom can be used as a qubit;

- Spin: the spin of the nuclei of atoms and molecules can be used as qubit.

- Superconductors: A superconducting LC circuit consists of an inductance and a capacitor connected by a superconducting wire, where current flows without resistance. When a Josephson junction is added to the circuit, the energy of the system can become quantized and the energy states can be manipulated to represent qubits. Superconducting qubits are among the most promising approcheas to building quantum computers.

1.1.2 Single qubit gates

In classical computing, where bits are the units of information, logic gates are the essential components for manipulating data and executing operations on them. The concept of logic gate can be extended and applied to quantum computation.

A quantum gate on a single qubit can be represented as a two by two unitary matrix U. Consider the qubit state $|\psi'\rangle$, obtained by the action of U on a qubit $|\psi\rangle$:

$$\left|\psi'\right\rangle = U\left|\psi\right\rangle = \alpha'\left|0\right\rangle + \beta'\left|1\right\rangle \tag{1.5}$$

The normalization condition must be true also for $|\psi'\rangle$: $|\alpha'|^2 + |\beta'|^2$ must be equal to one. It turns out that this condition is satisfied if the gate U is unitary, that is $U^\dagger U = 1$.

An important single qubit quantum gate is the NOT gate, represented by a matrix X such that

$$X = \begin{pmatrix} 0 & 1 \\ 1 & 0 \end{pmatrix} \tag{1.6}$$

$$X\begin{pmatrix} \alpha \\ \beta \end{pmatrix} = \begin{pmatrix} \beta \\ \alpha \end{pmatrix} \tag{1.7}$$

Another significant gate is the Z gate:

$$Z = \begin{pmatrix} 1 & 0 \\ 0 & -1 \end{pmatrix} \tag{1.8}$$

$$Z\begin{pmatrix} \alpha \\ \beta \end{pmatrix} = \begin{pmatrix} \alpha \\ -\beta \end{pmatrix} \tag{1.9}$$

Finally, one of the most useful quantum gates is the Hadamard gate H.

$$H = \frac{1}{\sqrt{2}} \begin{pmatrix} 1 & 1 \\ 1 & -1 \end{pmatrix} \tag{1.10}$$

When applied to the base states $|0\rangle$ and $|1\rangle$. the Hadamard gate acts as follows:

3

$$H|0\rangle = \frac{|0\rangle + |1\rangle}{2} \quad ; \quad H|1\rangle = \frac{|0\rangle - |1\rangle}{2} \tag{1.11}$$

In the Bloch sphere representation, it can be observed that single-qubit gates correspond to rotations and reflections of the sphere. For instance, the Hadamard gate action is a rotation of the sphere about the y-axis by 90°, followed by a rotation around the x-axis by 180°.

1.1.3 Multiple qubits

When two or more qubits are involved, their state space is the *tensor product* $\otimes$ of the single qubit Hilbert space. For example, given two qubits in the state $|1\rangle$, the state of the entire system is

$$|1\rangle \otimes |1\rangle = |11\rangle \tag{1.12}$$

A general two-qubits state is:

$$|\psi\rangle = \alpha_{00}|00\rangle + \alpha_{01}|01\rangle + \alpha_{10}|10\rangle + \alpha_{11}|11\rangle \tag{1.13}$$

$|00\rangle$, $|01\rangle$, $|10\rangle$ and $|00\rangle$ are the computational base states and their coefficients provide the probabilities of measuring each state. The condition that the total probability must sum up to one si expressed by the following normalization relation:

$$\sum_{x\in\{0,1\}^2} |\alpha_x|^2 = 1 \tag{1.14}$$

The tensor product between two vectors is obtained by multiplying each term of the first vector by the entire second vector. It is possible to obtain the basis of the multiple-qubit Hilbert space by calculating the tensor product between the base states of the single-qubit Hilbert space. For example, when two qubits are involved

$$|00\rangle = \begin{pmatrix} 1 \\ 0 \\ 0 \\ 0 \end{pmatrix} \quad |01\rangle = \begin{pmatrix} 0 \\ 1 \\ 0 \\ 0 \end{pmatrix} \quad |10\rangle = \begin{pmatrix} 0 \\ 0 \\ 1 \\ 0 \end{pmatrix} \quad |11\rangle = \begin{pmatrix} 0 \\ 0 \\ 0 \\ 1 \end{pmatrix} \tag{1.15}$$

Hence, the state defined in Equation 1.13 can be represented as

$$|\psi\rangle = \begin{pmatrix} \alpha_{00} \\ \alpha_{10} \\ \alpha_{01} \\ \alpha_{11} \end{pmatrix} \tag{1.16}$$

In general, for a system of n qubits, the base states are of the form $|x_1 x_2...x_n\rangle$, where $x \in \{0,1\}$, and the dimension of the Hilbert space is 2^n. The vector representation of a general state is

$$|\psi\rangle = \begin{pmatrix} \alpha_0 \\ \alpha_1. \\ . \\ . \\ \alpha_{2^n-1} \end{pmatrix} \tag{1.17}$$

4

For a multiple-qubit system, it is possible to measure one qubit at a time. For instance, measuring the first qubit of the state in Equation 1.13, gives 0 with probability $|\alpha_{00}|^2 + |\alpha_{01}|^2$ and the final state of the system is

$$|\psi'\rangle = \frac{\alpha_{00}|00\rangle + \alpha_{01}|01\rangle}{\sqrt{|\alpha_{00}|^2 + |\alpha_{01}|^2}} \tag{1.18}$$

Product states and entangled states

Some quantum states can be factored into individual qubit states. For example,

$$\frac{1}{2}(|00\rangle - |01\rangle + |10\rangle - |11\rangle) = \frac{1}{\sqrt{2}}(|0\rangle + |1\rangle) \otimes \frac{1}{\sqrt{2}}(|0\rangle - |1\rangle) = |+\rangle|-\rangle \tag{1.19}$$

Such states are called *product states* or *simply separable states*. However, there exist quantum states that can not be factored into product states, these are called *entangled states*. An example is the *Bell state*,

$$|\phi\rangle = \frac{1}{\sqrt{2}}(|00\rangle + |11\rangle) \tag{1.20}$$

In this scenario, measuring the first qubit results in the state $|00\rangle$ with probability $\frac{1}{2}$ and the state $|11\rangle$ with probability $\frac{1}{2}$. The measurement of the first qubit simultaneously determines the state of the second qubit. In contrast, as illustrated in Equation 1.18, when the first qubit collapses to $|0\rangle$, the state of the second qubit remains in a superposition. Furthermore, in Equation 1.20, measuring the second qubit would yield the same value of the first. This implies a correlation in the measurement outcomes.

1.1.4 Multiple-qubit gates

When the state system $|\psi\rangle$ is described by two or more qubits, the quantum logic gates acting independently on each qubit $|\psi\rangle$ can be written as tensor product of single-qubit gates. For instance,

$$HI|00\rangle = (H \otimes I)(|0\rangle \otimes |0\rangle) = H|0\rangle \otimes I|0\rangle = \frac{1}{\sqrt{2}}(|00\rangle + |10\rangle) \tag{1.21}$$

Multiple-qubit gates are quantum gates that operate on more the one qubit at the same time. An important two-qubit gate is the CNOT or *controlled-NOT gate*:

$$CNOT = \begin{pmatrix} 1 & 0 & 0 & 0 \\ 0 & 1 & 0 & 0 \\ 0 & 0 & 0 & 1 \\ 0 & 0 & 1 & 0 \end{pmatrix} \tag{1.22}$$

$$CNOT|A\rangle|B\rangle = |A\rangle|A \oplus B\rangle \tag{1.23}$$

There are many other interesting gates other than CNOT, however it can be proved that any multiple-qubit logic gate may be composed from CNOT and a finite set of single qubit gates, which are then the prototypes for all other gates. [16]

1.1.5 Quantum circuits

A quantum circuit can be represented as a network of horizontal lines and gates. These lines do not correspond to physical wires, but they coincide with qubits. The circuit is to be read from left to right. The gates are the items connected by wires, each performing an operation on the corresponding qubits:

$$\alpha\,|0\rangle + \beta\,|1\rangle \quad \boxed{X} \quad \beta\,|0\rangle + \alpha\,|1\rangle$$

$$\alpha\,|0\rangle + \beta\,|1\rangle \quad \boxed{Z} \quad \alpha\,|0\rangle - \beta\,|1\rangle$$

$$\alpha\,|0\rangle + \beta\,|1\rangle \quad \boxed{H} \quad \alpha\frac{|0\rangle+|1\rangle}{2} + \beta\frac{|0\rangle-|1\rangle}{2}$$

The CNOT gate action is:

$$|A\rangle \quad\bullet\quad |A\rangle$$
$$|B\rangle \quad\oplus\quad |A \oplus B\rangle$$
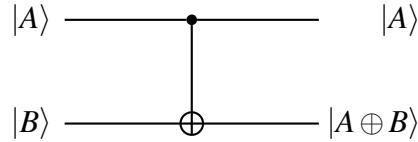
Finally, an important operation is measurement, which is represented by a "meter" symbol.

$$\boxed{H} \quad \overset{\beta}{\bullet} \quad \boxed{H} \quad \overset{|\pm\rangle}{\boxed{\nearrow}}$$
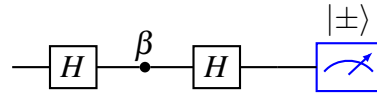
1.2 Stabilizer theory

1.2.1 Pauli matrices

The Pauli matrices are defined as:

$$\sigma_x = \begin{pmatrix} 0 & 1 \\ 1 & 0 \end{pmatrix} \quad \sigma_y = \begin{pmatrix} 0 & -i \\ i & 0 \end{pmatrix} \quad \sigma_z = \begin{pmatrix} 1 & 0 \\ 0 & -1 \end{pmatrix} \tag{1.1}$$

They are Hermitian matrices, all three of which have the same eigenvalues : $\lambda = \pm 1$. Some useful properties are:

- $\text{Det}(\sigma_j) = -1, \quad j = x, y, z;$

- $\text{Tr}(\sigma_j) = 0;$

- $(\sigma_x)^2 = (\sigma_y)^2 = (\sigma_z)^2 = I$

- $[\sigma_i, \sigma_j] = 2i\varepsilon_{ijk}\sigma_k$

Pauli matrices, along with the identity matrix I, constitute a basis for the space of two by two Hermitian matrices. These matrices represent any observable associated with a qubit.

In quantum computing, the Pauli matrices are associated with the X, Y, and Z gates, such as those defined in Equation 1.6 and 1.8.

An operator given by the tensor product of single-qubit Pauli operators and the identity I, is referred to as a *Pauli string*.

1.2.2 Quantum error correction

Modeling quantum noise

A physical system described in a quantum circuit is subject to noise. Even though the source of errors is diverse, a very general and simple noise model can be used in a variety of situations: the *Pauli error model* [19]. The basic idea of this model is that there are two types of errors that can be identified— *bit-flip errors* and *phase-flip errors*— and any error on a qubit can be expressed in terms of just these two.

A bit-flip error is given by the action of the gate X on the general qubit state 1.1.

$$X \ket{\psi} = \alpha \ket{1} + \beta \ket{0} \tag{1.2}$$

On the other hand, a phase-flip error is obtained by applying the Z gate to the state 1.1:

$$Z \ket{\psi} = \alpha \ket{0} - \beta \ket{1} \tag{1.3}$$

Encoding and decoding in quantum computing

To identify errors in a quantum circuit, the base states of a logical qubit are encoded using physical redundant qubits:

$$\ket{0} \to \ket{000}_e \quad \text{and} \quad \ket{1} \to \ket{111}_e \tag{1.4}$$

The encoded state is then

$$\ket{\psi}_e = \alpha \ket{000} + \beta \ket{111} \tag{1.5}$$

This encoding is called *3-repetition quantum code*, the encoded state is a *codeword* and the space of all codeword $\forall \alpha, \beta$ is a *codespace*.

Suppose that $\ket{\psi}_e$ goes through a noisy channel and a bit-flip error occurs. The final state is

$$\ket{\tilde{\psi}}_e = \alpha \ket{100} + \beta \ket{011} \tag{1.6}$$

In order to detect and correct this error, measurements on the state can be performed and, based on the measurements results, some correction operators can be applied.

In classical error correction, if an encoded bit $\ket{0}_e = \ket{000}$ is corrupted and becomes $\ket{\tilde{0}}_e = \ket{100}$, it is possible to directly measure each physical bit and a majority vote can be taken, revealing that the error occurred on the first bit.

However, in the case of a quantum system, measurements could cause the collapse of the system. Therefore, it is crucial to develop instruments that can prevent this outcome.

Stabilizers are operators with specific properties that can be employed to define codewords. These stabilizers can be measured without causing the collapse of the state, enabling the detection of errors and the restoration of the original state.

7

1.2.3 Stabilizers

The *Pauli group* P_n is the set of Pauli strings on n qubits, with the matrix multiplication as the group operation:

$$P_n = \{ \eta_i \mid \eta_i = \omega \sigma_1 \otimes ... \otimes \sigma_n, \ \sigma_j \in \{I, \sigma_x, \sigma_y, \sigma_z\}, \ \omega \in \{+1, -1, +i, -i\} \} \quad (1.7)$$

The multiplicative factors ± 1 e $\pm i$ are included because they ensure that P_n is close under multiplication.

In general, a group can be described by its generators [16]. A set of elements $g_1, \ldots, g_l$ in a group G is said to *generate* the group G if every element of G can be written as product of (possibly repeated) elements from the list $g_1, \ldots, g_l$, and it is written $G = < g_1, ..., g_l >$.

A *stabilizer group* S_n is an abelian subgroup of the Pauli group P_n that does not contain $-I$. This definition entails the following properties.

- since every element is a Pauli operator, each stabilizer has eigenvalues ± 1;

- it is a group, this implies that the product of two stabilizers is also a stabilizer;

- this group is abelian, meaning that any two stabilizers commute.

Moreover, given a physical system with the Hamiltonian H, if $S \in S_n$ is a symmetry of the system, the stabilizer S belongs to the class of quantum discrete symmetries, which are represented by a finite number of unitary (or anti-unitary) operators. In contrast to continuous symmetries, these operators are not continuous in the variables that describe the finite transformation. Examples of discrete symmetries are Z_2 symmetries, which include inversions, like *classical parity*. For a given quantum system, a symmetry is an inversion if it's described by a unitary operator such that $U^2 = I$. Stabilizers meet this last condition.

In quantum error correction, a stabilizer code is the common $+1$ eigenspace of all the operators in S_n. This vector space is referred to as the space V_{S_n} stabilized by the group S_n. When a stabilizer is measured, a result of -1 indicates that an error has occurred. It also possible to determine the error's location, by the combined measurement of multiple appropriately chosen stabilizers.

Stabilizers and unitary operators

Consider the vector space V_S stabilized by S_n and let $|\psi\rangle$ be any element of V_S. Suppose a unitary operator U is applied to $|\psi\rangle$, then

$$U|\psi\rangle = Ug|\psi\rangle = UgU^\dagger U|\psi\rangle \quad \forall g \in S_n \quad (1.8)$$

From this chain of equalities it can be deduced that the state $U|\psi\rangle$ is stabilized by $UgU^\dagger$:

$$UgU^\dagger U|\psi\rangle = U|\psi\rangle \quad (1.9)$$

Therefore, the group of stabilizers $US_nU^\dagger = \{UgU^\dagger | g \in S_n\}$, can be defined. Furthermore, if $g_1, \ldots, g_k$ are the generators of S_n, then $Ug_1U^\dagger, \ldots, Ug_kU^\dagger$ generate $US_nU^\dagger$.[16]

1.3 Qubit Tapering

1.3.1 Reducing symmetries to single Paulis

A n-qubit Hamiltonian can be expressed as

$$H = \sum h_i \eta_i \tag{1.10}$$

where h_i are real coefficients and η_i are elements of the Pauli group P_n.

The stabilizer group S_n is called the *symmetry of the Hamiltonian* if all elements of S_n commute with each Pauli term: suppose that $g_1, \dots, g_k$ are the generators of S_n, then

$$\left[g_j, \eta_i \right] = 0 \quad \forall i, j \tag{1.11}$$

This concept of symmetry is more restrictive than the conventional definition, which regards as symmetry any operator S that commutes with the Hamiltonian, i.e. $[S, H] = 0$.

According to equation 1.9, there exist a unitary operator U_i which maps the symmetry generators to single-qubit Pauli operators:

$$U_i g_i U_i^\dagger = \sigma_p^{(i)} \quad \forall i = 1, \dots, k \tag{1.12}$$

where (i) indicates the position of the qubit and $p \in \{1, 2, 3\}$, corresponding to the Pauli $\{\sigma_X, \sigma_Y, \sigma_Z\}$. The operator $\sigma_p^{(i)}$ acts trivially on $n-1$ qubits and with a single-qubit Pauli operator on the qubit at position i.

For each generator g_i, a transformation by U_i can be found. The unitary U_i can be constructed as a Clifford operator: the Clifford group on n qubits is the set of unitary operators U such that

$$U \gamma U^\dagger \in P_n \quad \forall \gamma \in P_n \tag{1.13}$$

Consider a subset of qubits $q_1, \dots q_k$ such that $\sigma_p^{(i)}$ anti-commutes with g_i and commutes with all the other generators $g_j \ \forall j \neq i$:

$$\sigma_p^{(i)} g_j = (-1)^{\delta_{ij}} g_j \sigma_p^{(i)} \tag{1.14}$$

This allows to define the unitary Clifford operators

$$U_i = \frac{1}{\sqrt{2}} (\sigma_p^{(i)} + g_i) \qquad i = 1, \dots, k \tag{1.15}$$

Using the commutation rules in 1.14, it can be shown that

$$U_i^2 = 1, \quad U_i \sigma_p^{(i)} U_i^\dagger = g_i, \quad U_j \sigma_p^{(i)} U_j^\dagger = \sigma_p^{(i)}, \forall j \neq i \tag{1.16}$$

and the transformation 1.12 can be obtained.

1.3.2 Removing qubits from the Hamiltonian

Let $\{|v_i\rangle\}$ be an orthonormal basis of the state space ε, assumed to be discrete. Consider the action of a unitary operator U on $|v_i\rangle$: $U|v_i\rangle = |\tilde{v}_i\rangle$. It can be shown that $\{|\tilde{v}_i\rangle\}$ form an orthonormal basis of ε. Given two operators $\tilde{A}$ and A, $\tilde{A}$ is the transform of A by U if $\langle \tilde{v}_i | \tilde{A} | \tilde{v}_j \rangle = \langle v_i | A | v_j \rangle$: $\tilde{A}$ and A have the same matrix elements on different basis. $\tilde{A}$ can

be obtained from A by the following relation:

$$\tilde{A} = UAU^{\dagger} \tag{1.17}$$

Therefore, the Hamiltonian H can be transformed using the Clifford operators U_i found in the previous step:

$$\tilde{H} = U_i H U_i^{\dagger} \tag{1.18}$$

Since S_n commutes with H as indicated by 1.11, it follows that the transformed operators still commute:

$$\left[\sigma_p^{(i)}, U \eta_i U^{\dagger} \right] = 0 \quad \forall i \tag{1.19}$$

This relation implies that the transformed term of the Hamiltonian, $U \eta_i U^{\dagger}$, acts by the Pauli operator σ_p on the ith qubit. The σ_p^i can be replaced with one of its eigenvalues, $+1$ or -1, and the associated qubit can be removed from the simulation. Therefore, the reduced Hamiltonian depends on the choice of the eigenvalue of σ_p.

Suppose k symmetry generators are found, then k qubits can be tapered off and the set of the chosen k eigenvalues is called *sector*. Overall, there are 2^k possible different sectors, each corresponding to a different Hamiltonian, related to specific properties and states of the system. For instance, one can study which sector corresponds to the ground state.

Moreover, it is important to notice that the operators obtained by the transformation 1.17 have the same eigenvalues:

$$A |\psi_a\rangle = a |\psi_a\rangle \Rightarrow \tilde{A} |\tilde{\psi}_a\rangle = (UAU^{\dagger})U |\psi_a\rangle = UA(U^{\dagger}U) |\psi_a\rangle = UA |\psi_a\rangle = aU |\psi_a\rangle = a |\tilde{\psi}_a\rangle \tag{1.20}$$

In consequence, the Hamiltonian H and its transform $\tilde{H}$ have the same eigenvalues. Hence, the tapering procedure explained above does not change the energy values of the system.

1.3.3 Tapering and quantum chemistry

An interesting area of research concerns the physical meaning of the symmetries of the system identified by the tapering procedure. [26]

In particular, when the physical system of interest is a molecule, it is possible to look for a correspondence between the generators of the symmetry defined in Equation 1.11 and point group symmetries.

A *point group* is a mathematical group of symmetry operations that have a fixed point in common, left unchanged. These operations are:

- *Proper rotation* (C_n): rotation by $360/n$ degrees;

- *Plane-reflection* (σ): reflection in a given plane;

- *Improper axis rotation* (S_n): rotation by $360/n$ followed by reflection in plane perpendicular to the rotation axis;

- *Center of inversion* (i): inversion of all atomic coordinates about the center

Moreover, there are two other interesting symmetries, beyond the point group ones[22]. In the non relativistic treatment of molecular systems, which doesn't consider effects like the spin-orbit interaction, the operators for the number of electrons with spin up ($\hat{N}_{\uparrow}$)

and spin down $(\hat{N}_\downarrow)$ are symmetries of the Hamiltonian. Consequently, so are the parity operators $(\hat{P}_\uparrow)$ and $(\hat{P}_\downarrow)$ defined by

$$(\hat{P}_\uparrow) = (-1)^{(\hat{N}_\uparrow)} \quad ; (\hat{P}_\downarrow) = (-1)^{(\hat{N}_\downarrow)} \tag{1.21}$$

If these two operators are multiplied together, they generate the total electron number parity symmetry, $\hat{P} = (-1)^{\hat{N}}$.

For a given molecule, specific algorithms can be employed to determine its point group symmetries. Subsequently, these symmetries can be represented in the qubits' Hilbert space. Generally, this representation is a summation of Pauli strings, which can ultimately be simplified into a single Pauli string.

It has been observed that certain symmetries obtained through this procedure coincide with those derived using the tapering technique, which are thus provided with physical meaning [26].

Chapter 2

In the realm of quantum mechanics, the concept of second quantization plays a fundamental role in understanding the behavior of identical particles. Second quantization provides a powerful framework for describing systems comprised of multiple identical particles, allowing us to analyze their collective behavior and interactions.

One notable application of second quantization theory is found in the Bose-Hubbard model, a fundamental model used to study the behavior of ultracold bosonic atoms confined in optical lattices. The Bose-Hubbard model captures essential aspects of the physics governing these systems, including the interplay between kinetic energy and interactions among the bosonic particles. It notably characterizes a quantum transition between a superfluid and insulator state.

In order to simulate a physical system, it is necessary to describe its model using qubits, which are which are the units of information of quantum computing. Therefore, the second quantization description of the Bose-Hubbard Hamiltonian must be mapped in the Hilbert space of qubits.

This mapping process involves encoding the relevant information about the system's state and dynamics into qubits, enabling quantum algorithms to simulate and manipulate the behavior of the system efficiently.

Two common encoding schemes employed in this mapping process are unary encoding and binary encoding.

2.1   Second quantization

Consider N identical particles and an arbitrary orthonormal basis $\{|u_k\rangle\}$ of the state space of a single particle. Based on the nature of the identical particles, the physical states of this system exhibit symmetry or anti-symmetry upon permutation. Those particles for which the physical states are symmetric are called *bosons*, and those for which they are anti-symmetric are *fermions*. Given the tensor product of single particle states,

$$\left|u_i^1, u_j^2, \ldots, u_p^N\right\rangle \tag{2.1}$$

in order to obtain the actual state of the system, the state 2.1 must be suitably symmetrized or anti-symmetrized. However, if the number of identical particles that constitutes the system is large, this operation leads to complex calculations. This description can be simplified in the Second Quantisation formalism, which provides a framework for the formulation of many-body quantum systems. [6]

2.1.1 Fock states and Fock space

The state of a system of N identical particles, can be described employing the concept of *occupation number*: by definition, given the state 2.1, the occupation number is the number n_k of particles in the state u_k. The state of the system can then be represented as

$$|n_1, n_2, \ldots, n_k, \ldots\rangle \tag{2.2}$$

where

$$n_1 + n_2 + \ldots + n_k = N \tag{2.3}$$

States such as 2.2 are called *Fock states*. Some of their properties are:

- the scalar product of two kets $|n_1, n_2, \ldots, n_k, \ldots\rangle$ and $|n'_1, n'_2, \ldots, n'_k, \ldots\rangle$ is different from zero only if all the occupation numbers are equal;

- if the particles under study are bosons, the kets $|n_1, n_2, \ldots, n_k, \ldots\rangle$, are characterized by occupation numbers n_i that can take on arbitrary values, provided that $\sum_{i=1}^{k} n_i = N$). The state space $F_S(N)$ includes the symmetric states of N particles.

- if the particles under study are fermions, the occupation numbers can either be 0 or 1. In this case, the state space $F_A(N)$ includes the anti-symmetric states of N particles.

When the number of particles of the system is variable, the *Fock space F* is introduced:

$$F = F(0) \oplus F(1) \oplus F(2) \oplus \ldots \oplus F(N) \oplus \ldots \tag{2.4}$$

$F(N)$ corresponds to the physical state space of N identical particles previously defined. It is possible to distinguish the Fock space for fermions, F_A, from that for bosons, F_S.

Since the Fock space F is obtained by a direct sum, the basis of F is obtained by combining the bases of all $F(N)$. A Fock state such as that defined in Equation 2.2 and 2.3 belongs to the subspace $F(N) \subset F$. $F(0)$ only contains the vacuum state $|0\rangle$.

An example of a system in which the total number of particles is not constant is the following:

$$|0\rangle + |1\rangle + |1, 1\rangle \tag{2.5}$$

This state (which should be suitably normalized) is the superposition of states with a different number of particles, 0, 1 or 2.

There are two operators that allow to navigate the Fock space: the *creation* and the *annihilation operators*, which respectively add and remove one particle to the system.

Bosonic creation and annihilation operators

For bosons, the *creation operator* on the state $|u_i\rangle$ is defined by:

$$a_i^\dagger |n_1, n_2, \ldots, n_i, \ldots\rangle = \sqrt{n_i + 1} |n_1, n_2, \ldots, n_i + 1, \ldots\rangle \tag{2.6}$$

It adds a particle to the system, which goes from a state of $F_S(N)$ to a state of $F_S(N+1)$.

Creation operators applied on the vacuum state allow to build occupied states:

$$|n_1, n_2, \ldots, n_i, \ldots\rangle = \frac{1}{\sqrt{n_1! n_2! ..n_k! ..}} \left[a_1^\dagger\right]^{n_1} \left[a_2^\dagger\right]^{n_2} .. \left[a_k^\dagger\right]^{n_k} .. |0\rangle \tag{2.7}$$

The *annihilation operator* on the state $|u_i\rangle$ is defined by:

$$a_i|n_1, n_2, \ldots, n_i, \ldots\rangle = \sqrt{n_i}|n_1, n_2, \ldots, n_i - 1, \ldots\rangle \tag{2.8}$$

This operator takes away one particle from the system and it yields zero when applied on a state where $|u_i\rangle$ is empty:

$$a_i|n_1, n_2, \ldots, n_i = 0, \ldots\rangle = 0 \tag{2.9}$$

The commutation relation of these operators are:

$$\left[a_i^\dagger, a_j^\dagger\right] = 0 \quad \left[a_i, a_j\right] = 0 \quad \left[a_i, a_j^\dagger\right] = \delta_{ij} \tag{2.10}$$

Finally, the *number operator* can be defined :

$$\hat{n}_i = a_i^\dagger a_i \tag{2.11}$$

In fact, if the creation and annihilation operators for bosons are successively applied to 2.2, one can observe that this operator yields the same Fock state, but multiplied by the number n_i.

2.2 The Bose-Hubbard model

2.2.1 The Hamiltonian

The Bose-Hubbard Hamiltonian is the following [25]:

$$H_{BH}/\hbar = -t \sum_{<i,j>} a_i^\dagger a_j + \frac{U}{2} \sum_i n_i(n_i - 1) - \mu \sum_i n_i \tag{2.12}$$

$a_i^\dagger$ and a_i are the creation and annihilation operators for site i, while n_i is the number operator and μ is the chemical potential.

The term

$$-t \sum_{<i,j>} a_i^\dagger a_j \tag{2.13}$$

can be interpreted as the kinetic energy of the system: the terms $a_i^\dagger a_j$ describe a particle moving from lattice site j, to lattice site i, with tunneling amplitude t. In this case, only nearest-neighbor hoppings are taken into account. It can be noticed that the negative sign preceding the term 2.13 alludes that a large hopping term is energetically favourable.

On the other hand, the term

$$\frac{U}{2} \sum_i n_i(n_i - 1) \tag{2.14}$$

corresponds to the potential energy associated with on-site particle interactions. If U is positive, having more than one particle per site implies an energy penalty, whereas if U is negative, the interaction becomes attractive, leading to an energy gain.

Finally, the third addend describes the total chemical potential energy: it accumulates μ amount of chemical potential energy for each boson in the lattice.

In general, the ground state of the system is studied for different values of the parameters μ/U and t/U.

2.2.2 Quantum phase transitions

A physical system can undergo a transformation after which its properties change drastically: a phase transitions has occured. For example, it may freeze or melt. This macroscopic change is due to microscopic thermal fluctuations, which, however, disappear when the temperature of the system approaches zero.

On the other hand, a quantum phase transition is a phase transition between different quantum phases, which are phases of matter at zero temperature. They are obtained by changing some parameters in the Hamiltonian of the system.

Studying quantum phase transitions is fundamental to understand the physical properties of many systems. Although quantum phase transitions occur at zero temperature, they can also be detected at extremely low temperatures, where thermal fluctuations are dominated by quantum fluctuations.

In the Bose-Hubbard model, quantum phase transitions are driven by the competition between the hopping and interaction terms of the Hamiltonian in Equation 2.12: the quantum phase of the system depends by the value of the parameters t and U. [14]

Superfluid: $t \gg U$

In general, there is no limit to the number of bosons that can occupy a single state. When a gas of bosons is cooled to temperatures near zero, a significant fraction of particles occupies the same lowest quantum state, and microscopic quantum mechanical phenomena, such as wavefunction interference, manifest at a macroscopic scale. This state is known as Bose-Einstein condensate.

When the tunneling term t in 2.12 dominates the Hamiltonian, eigenstates consists of single particle wavefunctions spread out over the entire lattice. Actually, the fact that interactions between bosons are insignificant leads to interesting properties and behaviours of the system.

Since the particles are bosons, in the ground state all particles occupy the same lowest-momentum state. The ground state wave function can be written as

$$|\psi\rangle = \left(\sum_i a_i^\dagger\right)^N |0\rangle \tag{2.15}$$

Moreover, the probability distribution for the local occupation number n_i on a single lattice site is poissonian, that is, its variance is given by $Var(n_i) = \langle n_i \rangle$. In this configuration, adding a particle to the system costs no energy, the state is compressible and the energy spectrum is gapless. The system is said to be in a *superfluid phase*.

Mott insulator: $t \ll U$

In this case, the hoppings from one site to the next become energetically expensive, and the system's ground state will instead consist of localized particles distributed in order to minimize the interaction term, depending on the parameters μ and U.

When $t = 0$, the Hamiltonian can written as

$$H_{BH}/\hbar = \frac{U}{2}\sum_i n_i(n_i - 1) - \mu \sum_i n_i = \sum_i \frac{U}{2}\left[\left(n_i - \left(\frac{1}{2} + \frac{\mu}{U}\right)\right)^2 - \left(\frac{1}{2} + \frac{\mu}{U}\right)^2\right] \quad (2.16)$$

By seeking the minimum of the system's energy with respect to $\partial H/\partial n_i$, the following results are obtained:

1. If $\frac{\mu}{U} < 0$, the ground state has no bosons;

2. When $0 < \frac{\mu}{U} < 1$, each site lattice has one boson;

3. generally, when $n_i < \frac{\mu}{U} < n_i + 1$, the ground state is characterized by $n_i + 1$ bosons per site.

Therefore, in this limit each boson is constrained to one site. Excitations on the ground state correspond to adding or removing one boson from a lattice site, requiring a finite amount of energy, respectively equal to $U\left(n_i - \frac{\mu}{U}\right)$ and $U\left(\frac{\mu}{U} - n_i\right)$. The energy spectrum is gapped, the system is a *Mott insulator*. [4]

The ground state is a product of local Fock states for each lattice site, at even filling n it is written as:

$$|\psi\rangle = \prod_i (a_i^\dagger)^n |0\rangle \quad (2.17)$$

Phase diagram

Starting from one of the Mott insulating phases, if the parameter t is increased slightly, since the system is gapped, one expects the system to stay in the same phase for a small but finite value of t. As t becomes large enough, the system will transition into the superfluid phase.

The phase diagram of the Bose-Hubbard model consists of Mott insulating lobes, each corresponding to different boson densities. The right-hand side of the graph represents the superfluid phase.
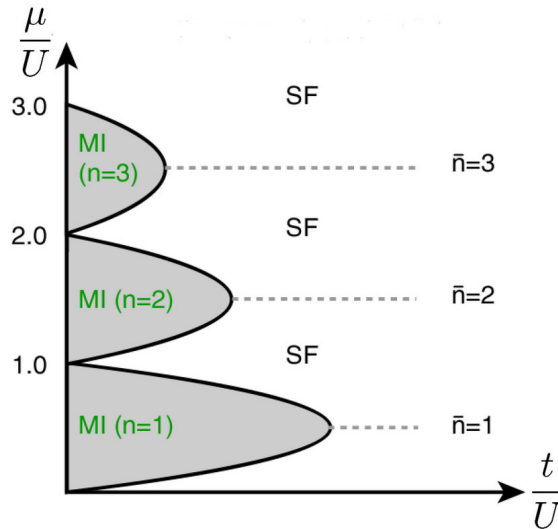

Figure 2.1: Bose Hubbard Phase Diagram.

2.2.3 U(1) symmetry in the Hamiltonian and superfluidity

Symmetry in the Hamiltonian and Spontaneous Symmetry Breaking

In quantum mechanics, a symmetry represents a collection of transformations of the state of a system that that leaves its physical observables unchanged [28]. This operations are described by unitary operators. A system is invariant with respect to a symmetry U if its Hamiltonian is also invariant:

$$H = U H U^\dagger \tag{2.18}$$

It follows that, as previously mentioned, the Hamiltonian commutes with the symmetry operator U:

$$[H, U] = HU - UH = 0 \tag{2.19}$$

However, U does not represent a physical observable, since in QM observables are described by hermitian operators. An important result from theory of Lie groups, states that given $U(\alpha_0, \ldots, \alpha_k)$ operator in k real parameters α_i, then

$$U(\alpha_0, \ldots, \alpha_k) = e^{i \Sigma_j \alpha_j T_j} \tag{2.20}$$

T_j are called *generators* of the group of transformations described by U. It can be proven that the generators are Hermitian, thereby representing physical quantities.

The relation between conservation laws and symmetries, can be understood considering the time evolution operator, which, for time independent Hamiltonians, is defined as $U(t) = e^{iHt}$. If $U = e^{iQ}$ is a symmetry of the system, it commutes with H and consequently it also commutes with $U(t)$. It follows that the expectation values of Q is constant in time. Since Q is hermitian, the observable Q is a constant of motion.

Moreover, the states of a system can also possess a symmetry. A system $|\psi\rangle$ is said to symmetric under a unitary transformation U if the obtained state is identical to the original, up to a phase:

$$U|\psi\rangle = e^{i\alpha}|\psi\rangle \tag{2.21}$$

Spontaneous symmetry breaking is a phenomenon in which a state of a system is not symmetric under a symmetry of its Hamiltonian[1]. In this case, H is invariant under U, but the state $|\psi\rangle$ is different from $U|\psi\rangle$. An immediate consequence is that the states $U|\psi\rangle$ and $|\psi\rangle$ have the same energy, which is degenerate.

Symmetry Breaking in the Bose-Hubbard Model

The Bose-Hubbard model conserves the number of bosons, since neither the kinetic energy term or the interaction and chemical potential terms change the number of bosons [5]. Therefore, the Hamiltonian 2.12 is invariant under the transformation

$$U_\alpha = e^{i\alpha \Sigma_k n_k} \tag{2.22}$$

where n_k is the single-site number bosonic operator defined in 2.26 and $\alpha \in [0, 2\pi)$. U_α forms a $U(1)$ symmetry group. This can be seen by the action of U_α on the creation and annihilation operators:

$$U_\alpha a_j^\dagger U_\alpha^\dagger = e^{i\alpha} a_j^\dagger \quad , \quad U_\alpha a_j U_\alpha^\dagger = e^{-i\alpha} a_j \tag{2.23}$$

$$\Rightarrow e^{i\alpha} a_j^\dagger e^{-i\alpha} a_k = a_j^\dagger a_k \quad \text{and} \quad e^{i\alpha} a_j^\dagger e^{-i\alpha} a_j = a_j^\dagger a_j \tag{2.24}$$

In the limit $t \gg U$, the ground state of the Bose-Hubbard model, breaks the symmetry of the Hamiltonian defined in Equation 2.22. In fact, in the superfluid phase, the ground state remains the same regardless of the number of particles in the system. The symmetry breaking is an additional characteristic that distinguishes the superfluid phase from the Mott insulator phase, which instead is symmetric.

2.3 Mapping to qubits

In order to simulate a quantum system on a quantum computer, it is necessary to represent theoretical models in terms of qubits and quantum gates. Moreover, the choice of a specific encoding for a given system is crucial for the computational cost of the simulation.

It must be emphasized that the encoding of bosons differs significantly from that of fermionic systems. For instance, fermionic occupation numbers are restricted to 0 or 1, establishing a direct correlation with the Hilbert space of qubits. Conversely, bosonic occupation numbers are not constrained and can assume any non-negative value. Additionally, in bosonic systems, there is no limit on the number of particles, necessitating the selection of a practical finite upper limit in actual simulations.

In the next sections, some bosons-to-qubit mappings are introduced [12], [18]. Consider a quantum system of bosons in a N-site lattice. Suppose that the maximum number of bosons in a single site is N_b, the state of this system is the Fock state

$$|n_1, \ldots, n_2, \ldots, n_N\rangle = |n_1\rangle \otimes |n_2\rangle \otimes \cdots \otimes |n_N\rangle \tag{2.25}$$

where the single particle state is identified by the site in the lattice where the particle is located.

The bosonic operators acting on the system are written as:

$$\begin{aligned}
\widetilde{a_i}^\dagger &= I \otimes \cdots \otimes a_i^\dagger \otimes \cdots \otimes I \\
\widetilde{a_i} &= I \otimes \cdots \otimes a_i \otimes \cdots \otimes I \\
\widetilde{n_i} &= I \otimes \cdots \otimes n_i \otimes \cdots \otimes I
\end{aligned} \tag{2.26}$$

I is the identity operator, while $a_i^\dagger$, a_i and n_i are the creation, annihilation and number operator associated to the ith site.

2.3.1 One-to-one mapping

The *one-to-one mapping*, also known as *unary mapping*, maps a boson state $|n_i\rangle$ to a tensor representation employing $(N_b + 1)$-qubit:

$$|n_i\rangle \leftrightarrow |0_0 \ldots 0_{n_i-1} 1_{n_i} 0_{n_i+1} \ldots 0_{N_b}\rangle \tag{2.27}$$

It is observed that adding a particle to the i-Th site corresponds to shifting the state $|1\rangle$ one position to the right: the qubit corresponding to the occupation number n_i becomes zero, while the one related to $n_i + 1$ becomes 1. Analogously, when a particle is removed from the ith site, it is expected that the state of the associated qubit becomes 0, while the one related to $n_i - 1$ becomes 1.

According to these considerations, the bosonic operators representations in this state space are:

$$
\begin{aligned}
I_i &= I_0 \otimes I_1 \otimes \cdots \otimes I_{N_b} \\
a_i^\dagger &= \sum_{n=0}^{N_b-1} \sqrt{n+1}\, I_0 \otimes \cdots \otimes \sigma_{+n} \otimes \sigma_{-n+1} \otimes \cdots \otimes I_{N_b} \\
a_i &= \sum_{n=1}^{N_b} \sqrt{n}\, I_0 \otimes \cdots \otimes \sigma_{-n-1} \otimes \sigma_{+n} \otimes \cdots \otimes I_{N_b} \\
n_i &= a_i^\dagger a_i
\end{aligned}
\tag{2.28}
$$

The multiplicative factors in the definitions of creator and annihilator are equal to those in 2.6 and 2.8, since the action on the state of the system is the same.

The operators σ_+ and σ_- are defined from the Pauli matrices:

$$
\begin{aligned}
\sigma_+ &= |0\rangle\langle 1| &&= \frac{1}{2}(X+iY) = \begin{pmatrix} 0 & 1 \\ 0 & 0 \end{pmatrix} \\
\sigma_- &= |1\rangle\langle 0| &&= \frac{1}{2}(X-iY) = \begin{pmatrix} 0 & 0 \\ 1 & 0 \end{pmatrix}
\end{aligned}
\tag{2.29}
$$

The unary mapping uses N_b+1 qubits for one site, corresponding to a state space with dimension 2^{N_b+1}. This mapping wastes a lot of resources, since most of these states do not have physical meaning. More efficient encodings can be defined.

2.3.2 Binary mapping

Binary mapping encodes a boson state in the binary representation of the occupation number:

$$
|n_i\rangle = |010\ldots110\rangle = |0\rangle_1 \otimes |1\rangle_2 \otimes \cdots \otimes |1\rangle_{N_q-1} \otimes |0\rangle_{N_q}
\tag{2.30}
$$

In consequence, single-site states are

$$
\begin{aligned}
|0\rangle &\leftrightarrow |0\rangle_1 \otimes |0\rangle_2 \otimes \cdots \otimes |0\rangle_{N_q-1} \otimes |0\rangle_{N_q} \\
|1\rangle &\leftrightarrow |0\rangle_1 \otimes |0\rangle_2 \otimes \cdots \otimes |0\rangle_{N_q-1} \otimes |1\rangle_{N_q} \\
|2\rangle &\leftrightarrow |0\rangle_1 \otimes |0\rangle_2 \otimes \cdots \otimes |1\rangle_{N_q-1} \otimes |0\rangle_{N_q} \\
&\;\;\vdots \\
\left|2^{N_q}-1\right\rangle &\leftrightarrow |1\rangle_1 \otimes |1\rangle_2 \otimes \cdots \otimes |1\rangle_{N_q-1} \otimes |1\rangle_{N_q}
\end{aligned}
\tag{2.31}
$$

According to this convention, the matrix representations of bosonic operators are:

$$
a_i^\dagger = \begin{pmatrix}
0 & 0 & 0 & \ldots & 0 & 0 \\
1 & 0 & 0 & \ldots & 0 & 0 \\
0 & \sqrt{2} & 0 & \ldots & 0 & 0 \\
\vdots & \vdots & \vdots & \ddots & \vdots & \vdots \\
0 & 0 & 0 & \ldots & \sqrt{2^{N_q}-1} & 0
\end{pmatrix}
\tag{2.32}
$$

19

$$a_i = \begin{pmatrix} 0 & 1 & 0 & \ldots & 0 & 0 \\ 0 & 0 & \sqrt{2} & \ldots & 0 & 0 \\ 0 & 0 & 0 & \ldots & 0 & 0 \\ \vdots & \vdots & \vdots & \ddots & \vdots & \sqrt{2^{N_q}-1} \\ 0 & 0 & 0 & \ldots & 0 & 0 \end{pmatrix} \tag{2.33}$$

$$n_i = \begin{pmatrix} 0 & 0 & 0 & \ldots & 0 & 0 \\ 0 & 1 & 0 & \ldots & 0 & 0 \\ 0 & 0 & 2 & \ldots & 0 & 0 \\ \vdots & \vdots & \vdots & \ddots & \vdots & \vdots \\ 0 & 0 & 0 & \ldots & 0 & 2^{N_q}-1 \end{pmatrix} \tag{2.34}$$

The bosonic operators defined above act in the same way as those in 2.6 and 2.8 on the Fock states.

The binary encoding allows for the representation of single-site Fock states with a maximum occupation number equal to $2^{N_q}-1$, using only N_q qubits, which all have physical meaning.

2.3.3 Truncation errors

The Fock space is infinite, and the bosonic creation operator can define states with one additional particle without limitations on the maximum number of bosons. Because of this, in the Bose Hubbard model, the occupation number of each site has no upper bound.

Moreover, the commutation relations presented in Equation 2.10 express some properties of the bosonic system. For instance, if the bosonic operators act on different states, their commutator is zero, according to the observation of their independence.

However, when the physical system is simulated on a quantum computer, the transition from the Fock space to the qubit Hilbert space leads to a truncation error: since only a finite number of qubits can be used, in order to represent the action of the bosonic operators in the qubit space, a finite upper limit on the number of bosons has to be selected. Then, this limit defines the number of qubits used in quantum simulations. If the physical system is composed of a large number of particles that has to be truncated, the consequent description and the results obtained will be approximated, since some physical states will be ignored.

The presence of truncation errors is made evident by computing the commutator of the matrices that represent the bosonic operators in the qubit space. Indeed, the relation $[a_i, a_j{}^\dagger] = \delta_{ij}$ is no longer valid.

Quantum states of the exact model with relatively low values of the occupation quantum number can be accurately approximated within the truncated model. However, as the system evolves according to the Hamiltonian H, the single-site occupation number may increase, surpassing the truncation threshold. As a result, even if the initial state is well approximated, this description may no longer be accurate after time evolution. To ensure that the truncated model can hold the evolved state, it is possible to constrain the rate of growth of the local occupation quantum number in the theoretical model. In addition, it can be taken into account the fact that states with fewer particles than the maximum allowed on each site evolve with small errors if the Hamiltonian conserves the total number.[18] [29]

Chapter 3

This chapter introduces a qubit-based implementation of the Bose Hubbard model Hamiltonian defined in Equation (2.12) and its optimization through Qubit Tapering.

In order to implement the Bose-Hubbard Hamiltonian, its terms need to be expressed as a summation of Pauli strings, as described in Equation (1.10). This approach allows the operator to act within the Hilbert space of qubits.

The simulation of the Bose Hubbard Hamiltonian is performed using Qiskit (Quantum Information Software Kit) [23], an open-source Python quantum computing software development kit (SDK) designed for creating experiments and programs.

A class called BoseHubbardHamiltonian is created, with methods enabling the construction of the Hamiltonian terms as sums of Pauli strings.

Once the Bose-Hubbard Hamiltonian for a specific system is obtained, Qubit Tapering is applied.

In this chapter, a system consisting of a linear lattice of three sites and two qubits per site is chosen as the model for the procedure.

The application of Qubit Tapering, as described in Section 1.3, relies on Symmer, a Python package for reducing qubit requirements in quantum computing. Symmer also provides tools for manipulating Pauli operators and quantum states [27]. Particularly, Qubit Tapering is implemented by the class QubitTapering.

Finally, the results obtained are analyzed. In general, according to Equation (1.20), it is expected that the energy spectrum of the system following tapering is equal to that of the initial Hamiltonian.

3.1 Implementation of the Bose Hubbard Hamiltonian

3.1.1 Lattices

To construct the Bose-Hubbard Hamiltonian for a given system, it is necessary to describe the characteristics of the lattice on which the bosons are located. Indeed, the behavior of the system's particles is related to how the lattice sites are connected to each other. Specifically, the definition of the kinetic term (2.13) of the Bose-Hubbard Hamiltonian indicates that bosons can only move from one site to another if they are adjacent, meaning there exists a connection between them.

In chemistry and physics, the *graph theory* is often employed to model systems such as molecules or interacting particles and to simulate their behaviors. Graphs are mathematical structures used to describe relations between pairs of objects. In this context, a graph is composed of vertices (also known as *nodes*) that are connected by edges (also known as *links* or *lines*) [30].

Therefore, in a physical lattice, the sites are represented by nodes, while the connections between them are described by edges. In the Bose Hubbard model (2.12), a boson can thus move between two connected nodes.

Qiskit-Nature is a package within the Qiskit framework, specifically designed to address quantum challenges in natural science applications. In particular, among other functionalities, it enables the implementation of physical lattices. [24]

In order to create and represent a lattice, the following modules must be imported.

```python
import numpy as np
import rustwork as rx
from qiskit_nature.second_q.hamiltonians.lattices import (
    BoundaryCondition,
    HyperCubicLattice,
    Lattice,
    LineLattice,
    SquareLattice,
    TriangularLattice,
)
```

In particular, *rustwork* is a Python library for working with graphs and graph theory, while classes such as *LineLattice*, *HypercubicLattice* and *SquareLattice* allow to build lattices of specific shapes and boundary conditions.

A very simple lattice is composed of *n* nodes distributed either as a line (open boundary conditions) or as circle (periodic boundary conditions).

```python
#line lattice implementation

num_nodes = 10 #number of sites in the lattice

boundary_condition = BoundaryCondition.OPEN #open lattice
#for closed lattices -> BoundaryCondition.PERIODIC

line_lattice = LineLattice(num_nodes=num_nodes, boundary_condition=
    boundary_condition)

line_lattice.draw()
```
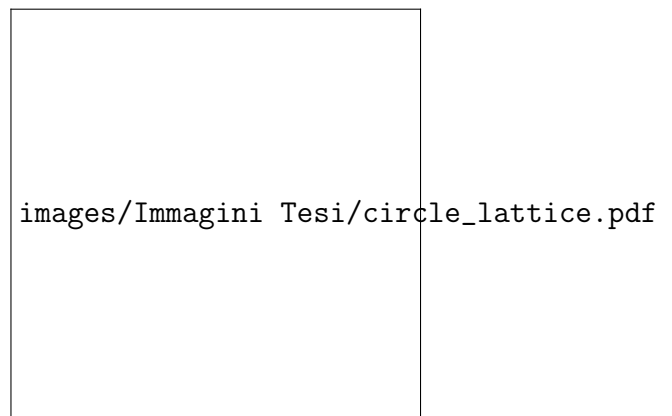

Figure 3.1: Open line lattice.

Figure 3.2: Closed line lattice.

The SquareLattice and TriangularLattice classes allow the creation of lattices with a fundamental unit of respectively four and three nodes.

Lattices with generic connections can also be obtained. To implement a general lattice an object, an instance of the rustwork class *PyGraph*, must be defined.

```
graph = rx.PyGraph(multigraph=False)   # multigraph shoud be False
graph.add_nodes_from(range(4))
edge_list = [
    (1, 0, 1.0),
    (1, 2, 1.0),
    (1, 3, 1.0),
]
graph.add_edges_from(edge_list)

# make a lattice
general_lattice = Lattice(graph)
```

By default a PyGraph is a multigraph, meaning that there can be parallel edges between nodes. However, in the case of the Bose-Hubbard model, there exists only one type of connection between adjacent nodes, and a single edge is adequate to describe the hopping of particles. The elements of the edge list are tuples containing three terms, the two nodes to be connected and the weight of the edge.
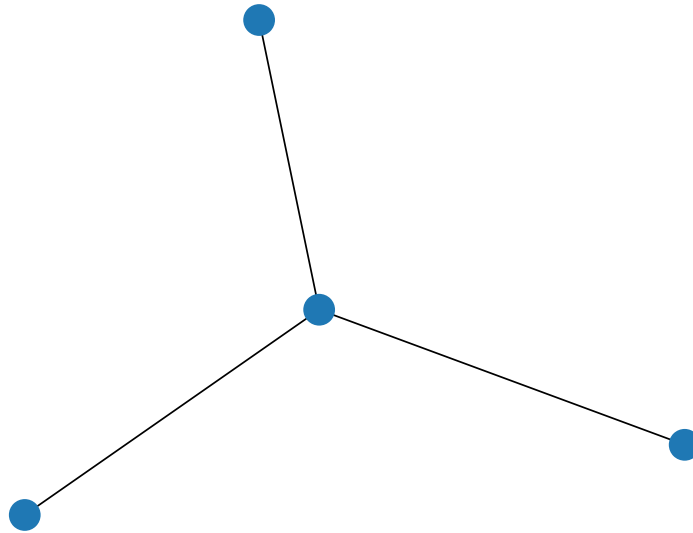

Figure 3.3: Example of generic lattice.

Finally, it is possible to model three-dimensional lattices, using a syntax like the following:

```
size = (3, 4, 5)
boundary_condition = (
    BoundaryCondition.OPEN,
    BoundaryCondition.OPEN,
    BoundaryCondition.OPEN,
)
cubic_lattice = HyperCubicLattice(size=size, boundary_condition=
    boundary_condition)
```

Functions that fix the positions of nodes in space can also be implemented and a lattices such that in 3.4 can be obtained.
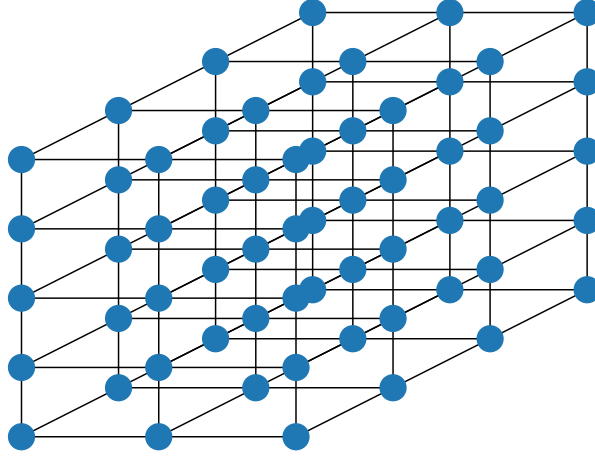
Figure 3.4: Example of Hypercubic lattice.

One important property of lattices, particularly in this work, is the *adjacency matrix* , a square matrix whose elements indicate whether two nodes are connected (are adjacent).

$$\begin{pmatrix} 0 & 1 & 0 & 0 \\ 1 & 0 & 1 & 1 \\ 0 & 1 & 0 & 0 \\ 0 & 1 & 0 & 0 \end{pmatrix} \qquad (3.1)$$

In Equation 3.1, the adjacency matrix of the lattice represented in Figure 3.3 is shown. The entries of the matrix are all zero except for the elements ij such that there exists an edge between nodes i and j. This matrix is symmetric, as a connection between node i and node j is the same as between node j and i. Additionally, the diagonal entries of the adjacency matrix represent self-connections. In Equation 3.1, the diagonal entries are zero because self-loops are not included in the lattice definition. However, in general, the adjacency matrix of an object such as LineLattice also contains self edges.

3.1.2 The Hamiltonian

Initialization

The implementation of the Bose-Hubbard Hamiltonian in the qubit Hilbert space is based on the Qiskit module *qiskit.quantum_info*. In particular, the classes *Pauli*, *SparsePauliOp* and *Operator* are used.

```
import math
import numpy as np

from qiskit.quantum_info import Pauli, Operator
from qiskit.quantum_info import SparsePauliOp
```

Initializing an instance of the class requires three parameters: the number of sites, the number of qubits used to describe the state of a single site and the lattice of interest.

The initialization of the object is the following:

```
class BoseHubbardHamiltonian:

    def __init__(self, n_sites, single_site_qubits, geometry):
```

```
4
5      # n_sites (int, n_sites >= 2)
6      # single_site_qubits (int)
7      # geometry (LineLattice or another type of lattice)
8
9          self.n_sites = n_sites
10         self.ss_q = single_site_qubits
11         self.geometry = geometry.to_adjacency_matrix()
12
13         self.total_number = None #initialization total_number
14
15          # call methods to initialize attributes
16         self.second_quantization_ops()
17         self.lattice_connectivity()
18         self.kinetic_energy_op()
19         self.potential_energy_op()
```

Single site bosonic operators

Recall the Bose-Hubbard Hamiltonian defined in Equation 2.12. The physical system is composed of N_b bosons in motion across N lattice sites, therefore the state of the system is 2.25. Using the binary encoding, the single site bosonic operators are those defined in 2.32, 2.33 and 2.34. Then, the operators on the *Nth*-site state can be obtained by appropriate tensor product.

If M is the number of qubits that describe each site, the qubit representation of the bosonic operators can be written as summation of Pauli strings utilizing *SparsePauliOp*, a method that allows writing an $N \times M$ -qubit operator as a list of $N \times M$ -qubit Pauli strings and complex coefficients. The construction of the creation and annihilation operators mapped to qubits is performed by the function *second_quantization_ops()*.

```
1   #creation, annihilation, number and identity operators on
      single_site_qubits number of qubits
2
3    def second_quantization_ops(self):
4
5        dim =  2**(self.ss_q)
6        create_matrix = np.zeros((dim,dim),dtype=float)
7
8        for i in range(dim-1):
9            create_matrix[i+1][i] = math.sqrt(i+1)
10
11       I_q_matrix = np.eye(dim, dtype=float)
12       I_q_Op = Operator(I_q_matrix)
13
14       # from matrix to Operator and from Operator to SparsePauliOp
15       createOp = Operator(create_matrix)
16       self.create = SparsePauliOp.from_operator(createOp)
17
18       self.annihilate = self.create.adjoint()
19       self.number = self.create.compose(self.annihilate).simplify
   ()
20
21       self.I_q =  SparsePauliOp.from_operator(I_q_Op))
```

Given the number of qubits per site M, the bosonic operators matrices have dimensions $2^M \times 2^M$. To construct the creator matrix 2.32, a zero matrix is defined at line 6 and subsequently filled with $\sqrt{n_i + 1}$ according to Equation 2.6. The identity matrix also

is defined. Following that, the creator matrix and the identity are converted to *Operator*, a class for representing matrix operators. This step is useful because it allows obtaining the representation of an operator as a list of Pauli strings through the method *SparsePauliOp.from_operator()*. This is what is done at lines 16 and 21. Moreover, the annihilation operator is obtained as adjoint of the creator, while the number operator is the composition of creator and annihilator, based on 2.11.

Hopping term

In the construction of the kinetic term 2.13, the lattice connectivity information is encoded within an appropriate adjacency matrix.

Once the single-site bosonic operators have been constructed, it is time to build the kinetic and potential terms, defined in 2.13 and 2.14.

The addends in the kinetic term of the Hamiltonian represent the displacement of a particle from site j to site i, where i and j are adjacent sites in the lattice. For entries ij in the connectivity matrix that equal 1, the operator $a_i^\dagger a_j$ acts on the state $|n_i\rangle \otimes |n_j\rangle$, while the states of other sites remain unchanged. Depending on indices ij, the addends constituting the kinetic energy have the following form:

$$I_1 \otimes I_2 \otimes \ldots a_i^\dagger \ldots a_j \ldots \otimes I_{N-1} \otimes I_N \tag{3.2}$$

where N is the number of sites in the lattice and the subscripts in $I_k \ \forall k = 1, \ldots, N$ indicate the site on which each operator acts.

```
def kinetic_energy_op(self):

    Op = []
    for i in range(self.n_sites):
        Op.append(self.I_q)

    kin = []
    for i in range(self.n_sites):
        for j in range(self.n_sites):

            if self.geometry[i][j] == 1:
                Op[i] = self.create
                Op[j] = self.annihilate

                Operator = Op[0]

                for k in range(1, self.n_sites):
                    Operator = Operator ^ Op[ k ]

                kin.append(Operator)

                Op[i] = self.I_q
                Op[j] = self.I_q

    self.Kinetic = sum(kin).simplify()
    return self.Kinetic
```

Interaction term

The simulation of the interaction term is similar to that of kinetic energy. In this case, each term is characterized by the presence of the single-site number operator:

$$\tilde{n}_i = I_1 \otimes \cdots \otimes \hat{n}_i \otimes \cdots \otimes I_N \tag{3.3}$$

$\tilde{n}_i$ is the operator associated with the ith site, which acts on the total state 2.25. Each addend is given by composition of $\tilde{n}_i$ and $(\tilde{n}_i - I_N)$ where I_N is the identity on a state of N sites, such 2.25.

The construction of the potential energy term is carried out in the following code:

```python
def potential_energy_op(self):

    I_n_list = []
    Op = []
    for i in range(self.n_sites):
        I_n_list.append(self.I_q)
        Op.append(self.I_q)

    #identity for n sites ss_q qubits per site
    I_n = I_n_list[0]
    i = 1
    while i < self.n_sites:
        I_n = I_n^I_n_list[i]
        i = i+1

    self.I_n = I_n

    number_tot = []
    potent = []
    for i in range(self.n_sites):
        Op[i] = self.number

        Operator = Op[0]

        for k in range(1, self.n_sites):
            Operator = Operator^Op[k]

        number_tot.append(Operator)

        Op[i] = self.I_q

    self.total_number = sum(number_tot)

    for i in range(self.n_sites):
        potent.append( number_tot[i].compose(number_tot[i] -
    self.I_n))

    self.Potential = sum(potent).simplify()

    return self.Potential
```

The complete Hamiltonian

Finally, the entire Hamiltonian as summation of Pauli strings can be obtained using the method *get_H()*:

```
1    def get_H(self, J, U):
2
3        self.U = U
4        self.J = J
5        H =  J*self.Kinetic + U*self.Potential
6        return H
7
```

In the code below, an example of defining an instance of the BoseHubbardHamiltonian class is shown. This system consists of a lattice with three sites having open boundary conditions, each containing two qubits. It will be utilized in the subsequent analysis of this work to apply Qubit Tapering and examine its outcomes.

```
1
2    num_qubits = 2
3    num_nodes = 3
4
5    H_instance = BoseHubbardHamiltonian(num_nodes, num_qubits,
     line_lattice)
6    H_q = H_instance.get_H(1,2)
7
```

3.2 Tapering off qubits

Consider a lattice system comprising three sites, with two qubits describing each site, along with its Hamiltonian, which was initialized in the preceding section.

Firstly, the Hamiltonian obtained by the BoseHubbardHamiltonian class is a *SparseP-auliOp* object and it must be converted into an instance of *PauliWordOp*, a class used to describe generic linear combinations of Pauli operators in Symmer. Such objects are those handled by QubitTapering methods.

This transformation is performed by the following instruction:

```
#Hamiltonian to be tapered
H = PauliwordOp.from_qiskit(H_q)
```

Then the Hamiltonian *H* has the form:

```
 0.933+0.000j  IXIXII +
 0.483+0.000j  IXXXII +
 0.483+0.000j  IXYYII +
-0.250+0.000j  IXZXII +
 0.933+0.000j  IYIYII +
-0.483+0.000j  IYXYII +
 0.483+0.000j  IYYXII +
-0.250+0.000j  IYZYII +
 0.483+0.000j  XXIXII +
 0.250+0.000j  XXXXII +
 0.250+0.000j  XXYYII +
 ...
```

Following that, according to Paragraph 1.3.1, the first step of the Tapering procedure is to find a symmetry of the system and its generators.

The procedure for finding such symmetry is based on the following reasoning. [26] Pauli operators can be represented as binary strings $(a_x|a_z)$ [7]. A Pauli operator is then obtained by

$$\eta(a_x|a_z) = \left(\prod_{i \in a_x} \sigma_x^i\right) \cdot \left(\prod_{j \in a_z} \sigma_z^j\right) \tag{3.4}$$

Indeed, the Pauli matrix σ_y can be obtained combining σ_x and σ_y: $\sigma_y = i\sigma_x\sigma_z$.

This parameterization is highly effective for multiplying two Pauli strings or for verifying their commutativity:

$$\eta(a_x|a_z)\eta(b_x|b_z) = (-1)^{a_x b_x + a_z b_z}\eta(b_x|b_z)\eta(a_x|a_z) \tag{3.5}$$

The two operators commute if $a_x b_x + a_z b_z = 0$ (mod 2). All the Pauli strings that appear in the Hamiltonian 1.10 can be represented as a binary matrix

$$G = (G_x \quad G_z) \tag{3.6}$$

where the jth line coincide with $(a_x|a_z)$ representing η_j. The symmetry elements correspond to the kernel of *G* matrix.

Once the generators g_i are found, each of them is mapped to a single-qubit Pauli operator $\sigma_p^{(i)}$, according to 1.12:

```
IndependentOp.symmetry_generators(H)

taper_hamiltonian = QubitTapering(H)
```

29

```
4        taper_hamiltonian.stabilizers.rotate_onto_single_qubit_paulis()
```

For the system under consideration, one symmetry generators is obtained:

```
1 #symmetry generators
2 IZIZIZ
3
4 #transformed generators
5 - IXIIII
```

At last, the operator $\sigma_p^{(i)}$ in the transformed Hamiltonian 1.18 can be replaced by ± 1 and the respective qubit can be dropped. In general, to each symmetry generator corresponds one qubit that can be removed.

The method *taper_it()* is responsible for the qubit reduction:

```
1        #sec_array= set of eigenvalues that replace the single-qubit
         Pauli
2        sec_array = [1] #otherwise [-1]
3
4        ham_tap = taper_hamiltonian.taper_it(sector=sec_array)
```

In the next code snippet, the reduced Hamiltonian related to $+1$ is printed. It can be observed that, while the initial Bose-Hubbard Hamiltonian is composed of six-qubit Pauli strings, the tapered Hamiltonian is characterized by 5-qubit Pauli strings. Indeed, one symmetry generator was identified for the Hamiltonian of the system.

```
1        6.000+0.000j IIIII +
2        1.000+0.000j IIIIZ +
3       -1.000+0.000j IIIZI +
4       -2.000+0.000j IIIZZ +
5        1.000+0.000j IIZII +
6        1.000-0.000j IIZIZ +
7       -1.000+0.000j IZIII +
8       -2.000+0.000j IZZII +
9       -1.000+0.000j ZIIII +
10      -2.000+0.000j ZIZIZ +
11      -0.933+0.000j IIXII +
12       ...
```

3.3 Analysis of results

3.3.1 The symmetries of the system and Tapering

The implementation and application of the Tapering procedure described in Section 3.2 was successful: the Bose-Hubbard Hamiltonian for bosons in a specific lattice can be represented using one fewer qubit. The symmetry that enables this reduction remains the same regardless of the type of lattice, for any value of t and U.

For the three-site lattice described by two qubits per site, such symmetry has the following form:

$$IZIZIZ \tag{3.7}$$

According to the Tapering theory, this symmetry is specifically a stabilizer that commutes with each addend of the Hamiltonian expressed as 1.10.

The physical interpretation of the operator 3.7 can be understood by observing the effect of the string

$$II \ldots IZ \tag{3.8}$$

on a single-site state. The binary mapping represents the number of bosons in a site using the base-2 numeral system. In this representation, the rightmost digit determines whether the number of bosons is even or odd. If it is 1, the number is odd; if it is 0, the number is even. The action of the Z operator on a qubit is described in Equation 1.9:

$$Z|0\rangle = |0\rangle \quad \text{and} \quad Z|1\rangle = -|1\rangle \tag{3.9}$$

Therefore, given a single-site state $|\psi\rangle$ binary representation with n_i bosons, the operator 3.8 is such that

$$\begin{cases} II \ldots IZ |\psi\rangle = +|\psi\rangle & \text{if } n_i \text{ is even} \\ II \ldots IZ |\psi\rangle = -|\psi\rangle & \text{if } n_i \text{ is odd} \end{cases} \tag{3.10}$$

Considering all sites of the lattice, the tensor product of the operators 3.8 has an eigenvalue of +1 if the number of particles in the system is even, and -1 if it is odd.

Since the operator 3.7 and its generalization to any number of qubits and sites is a symmetry of the system, there must be a corresponding conserved quantity: the parity of the number of particles in the system.

As stated in Section 2.2.3, the Bose-Hubbard Hamiltonian conserves the total number of bosons in the system, and the associated symmetry is given by 2.22. The symmetry identified by the Tapering procedure is a Z_2 symmetry and corresponds to $\alpha = \pi$.

The Bose-Hubbard model for a specific lattice possesses symmetries beyond the parity of the number of particles in the system. For example, the particle exchange operator is a symmetry of the Hamiltonian H in the sense that it commutes with H. This operator exchanges the particles located at one site of the lattice with those at another site. This action corresponds to swapping the positions of the two sites in space, and it is accomplished by appropriately combining the effects of swap matrices on the qubits that describe each site.

The two-qubits swap matrix is defined as following:

$$\begin{pmatrix} 1 & 0 & 0 & 0 \\ 0 & 0 & 1 & 0 \\ 0 & 1 & 0 & 0 \\ 0 & 0 & 0 & 1 \end{pmatrix} \tag{3.11}$$

In quantum computing the matrix 3.11 corresponds to the SWAP gate, whose action is

$$SWAP\,|01\rangle = |10\rangle \quad SWAP\,|10\rangle = |01\rangle, \tag{3.12}$$

while states $|00\rangle$ and $|11\rangle$ remain unchanged.

The two-qubits SWAP gate can be written as

$$SWAP = \frac{1}{2}\left(II + XX + ZZ + YY\right) \tag{3.13}$$

In the three-site/two-qubit-per-site system, the extension of the site exchange operator involves first swapping the first qubit of site 1 with the first qubit of site 3, followed by swapping the second qubit of site 1 with the second qubit of site 3.:

$$SWAP_1 = \frac{1}{2}\left(IIIIII + XIIIXI + YIIIYI + ZIIIZI\right) \tag{3.14}$$

$$SWAP_2 = \frac{1}{2}\left(IIIIII + IXIIIX + IYIIIY + IZIIIZ\right) \tag{3.15}$$

This site exchange symmetry commutes with the Hamiltonian H, but it does not commute with each term of 1.10, making it unsuitable for Qubit Tapering. This is true regardless of the number of sites or qubits in the system.

Furthermore, it is noted that geometric symmetries within the lattice do not lead to the removal of qubits. Regardless of the regularity of the lattice being studied, the tapering procedure does not identify geometric symmetries like rotations or reflections as useful for qubit elimination. This is due to the fact that geometric symmetries can be broken down into a series of transpositions, each exchanging two elements at a time. However, as mentioned before, these transformations cannot be utilized in tapering.[26]

3.3.2 Eigenvalues of the original and tapered Hamiltonians

To confirm the success of the Tapering procedure, the eigenvalues of the original Hamiltonian can be compared to those of the tapered Hamiltonian. According to 1.20, the initial Hamiltonian H and the transformed Hamiltonian $\tilde{H}$, given by 1.18, have the same eigenvalues. The eigenvalues of $\tilde{H}$ are obtained by combining the sets of the eigenvalues of the tapered Hamiltonian for each possible sector. In general, as mentioned in paragraph 1.3.2, if k is the number of qubits that can be removed, then there are 2^k sets of eigenvalues to be considered.

In the case of the three-site/two-qubit per site system under consideration, one qubit is eliminated, thus leading to two tapered Hamiltonians.

To perform this analysis, one can leverage the functionalities of SciPy, a Python module that provides advanced features for scientific and technical computing. In particular, the function *scipy.linalg.eigvals()* allows to calculate the eigenvalues of a given matrix.

A BoseHubbardHamiltonian instance is created for various values of the energy parameters t and $U = 1 - t$. The eigenvalues of the original Hamiltonian are collected into a matrix. Then, for each value of t, the Qubit Tapering procedure is performed, both substituting $\sigma_p^{(i)}$ in the transformed Hamiltonian 1.18 with $+1$ and -1. The eigenvalues of the two tapered Hamiltonians are then collected separately.
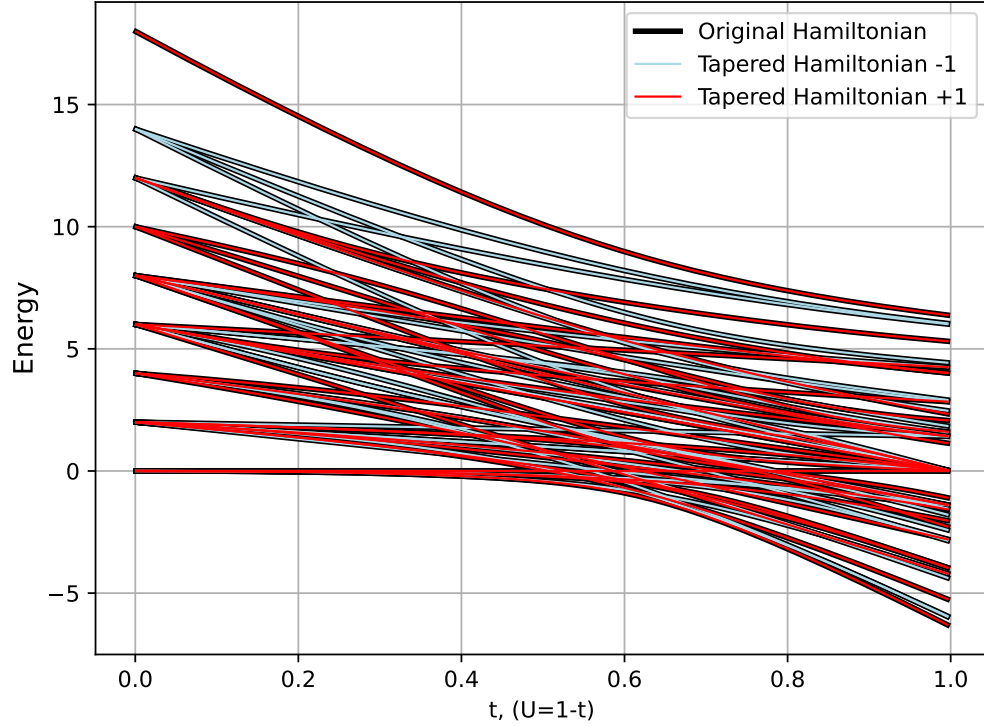
Figure 3.5: Comparison between eigenvalues of the original and tapered Hamiltonians for the Bose-Hubbard model with three sites.

The sets of calculated eigenvalues are then be displayed on the following graph.

As expected, Figure 3.5 illustrates that the energy spectrum of the tapered Hamiltonian, represented by the blue and red dashed lines, corresponds to that of the initial Hamiltonian (black continuous line).

It is important to note that not all eigenvalues of the Bose-Hubbard Hamiltonian are associated with eigenvectors representing physical states of an actual bosonic system. In fact, each site cannot contain more bosons than those expressed by the number of qubits employed and the dynamics of the system must adhere to this rule. Only those states such that the expectation value of the total number of particles operator is at most equal to the maximum number of bosons encoded in a lattice site can be considered as being correct approximations of the complete physical system.

A code similar to the one used to compare the eigenvalues of the initial and tapered Hamiltonians can be implemented to determine the energy spectrum of the Bose-Hubbard Hamiltonian using its corrected eigenstates. The system Hamiltonian is defined for various values of the hopping term t and the eigenvalues of H are then compared to the eigenvalues of a constrained Hamiltonian defined as

$$H_{const} = H + e \cdot (N_{tot} - N)^2 \tag{3.16}$$

where e is a real parameter at least equal to the difference between the maximum and the minimum eigenvalues of H, $N_{tot} = \sum \hat{n}_i$ and N is the selected number of particles in the system. In the case of two qubits per site, $N = 0, 1, 2, 3$.

As N varies, only the eigenvalues of H_{const} corresponding to eigenstates with a total

number of particles equal to N will remain equal to the initial eigenvalues of H. Otherwise, they are greater than the latter by at least e.

Figure 3.6 shows the energy spectrum of the Bose-Hubbard Hamiltonian relative to those states that satisfy the approximation, for different values of the parameters t and U.
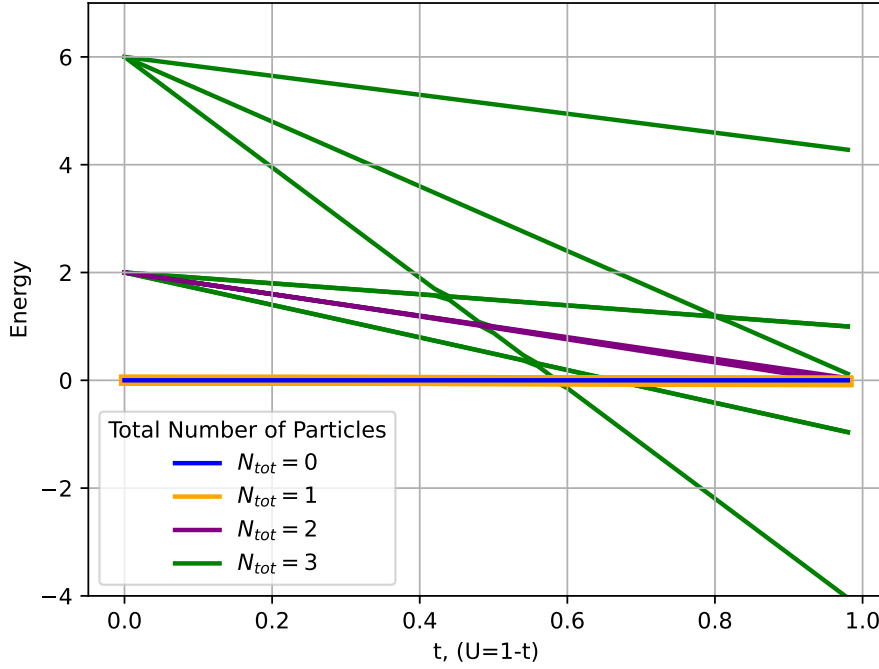

Figure 3.6: The energy spectrum of the Bose-Hubbard System in accordance with the system's approximation.

It is interesting to note that this graph reflects some characteristics of the spectrum of the Bose-Hubbard Hamiltonian described in Section 2.2. At $t = 0$, the system is characterized by discrete energy levels determined by the number of particles at each site: in this case, $U > 0$ so the higher the number of particles at each site, the higher the energy of the system, which is in the Mott insulator phase.

Conclusions

The present study aimed to analyze and apply a mathematical-computational method, Qubit Tapering, designed to reduce the computational resources required by a quantum computer for simulating physical systems.

Tapering applies the stabilizer formalism to perform qubit reduction. Indeed, it has been demonstrated how one can leverage the properties of stabilizers to eliminate qubits from the description of a system without compromising the accuracy of the simulation.

The system under consideration for the application of Tapering consisted of bosons in a lattice, described by the Bose-Hubbard model. The Qiskit framework allowed the description of such system in the Hilbert space of qubits. Various types of lattices were examined to explore the generality and applicability of the Tapering procedure. Regardless of the number of sites or bosons and the geometry of the lattice, the application of Tapering always yielded the same outcome. Therefore, the analyses were presented with reference to a particular model system, focusing on a three-site lattice scenario with each site described by two qubits, resulting in a maximum of three bosons.

By applying the Tapering procedure, one qubit could be effectively eliminated, achieving the goal of this thesis work. Initially represented by Pauli strings acting on a state space of dimension N (where N is the product of the number of qubits per site and the total number of sites), the Bose Hubbard Hamiltonian could then be described using $N - 1$ qubits. This reduction halved the dimension of the Hilbert space of qubits, thereby reducing the computational complexity of the system.

The symmetry operator utilized in qubit removal corresponded to the parity of the number of particles in the lattice, which is a conserved quantity of the system.

The theory of Tapering has raised questions about the relationship between the symmetries of the physical system and the stabilizers suitable for qubits removal. It has been understood that although the physical system may possess various symmetries, many of them either are not stabilizers or do not commute with all the Pauli strings that describe the Hamiltonian. For this reason, in the examined system, only one generator was identified.

The investigation of the energy spectrum of the system further validated the success of the Tapering procedure. The coincidence between the eigenvalues of the original and reduced Hamiltonians confirmed the preservation of the energy spectrum, demonstrating the reliability of the Tapering method in maintaining the essential characteristics of the system. Tapering is indeed a method that preserves the eigenvalues of the Hamiltonian considered in the study.

Furthermore, the correlation between the numerically obtained energy spectrum and the properties of different states described by the Bose-Hubbard model provided valuable insights into the behavior of the system under various conditions. In particular, the discrete energy spectrum of the Mott insulator phase could be observed by plotting the eigenvalues of the Hamiltonian for different values of the hopping and interaction parameters.

It is natural to wonder whether it is possible to develop methods and tools that allow

for further reduction of the computational resources required for describing the problem.

In this regard, it could be valuable to search for alternative mappings beyond the unary and binary mappings presented in this thesis, seeking approaches that could describe a bosonic physical system more efficiently.

In addition, the notion of qudits in quantum computing could be explored. Qudits, which consists of multi-level quantum states, offer a broader state space compared to traditional qubits, potentially enabling more efficient representation and manipulation of quantum information . Moreover, the qubit stabilizer theory has already been extended to qudits [10]. By extending the principles of Tapering to qudits, specific operations could be devised to reduce the number of qudits required for system description without compromising simulation accuracy. Leveraging the system's symmetries in this context could be instrumental in effectively reducing the dimensionality of the state space, thereby enhancing the efficiency of quantum simulations.

Bibliography

[1] Aron J. Beekman, Louk Rademaker, and Jasper van Wezel. *An introduction to spontaneous symmetry breaking*. SciPost foundation, 2019.

[2] Sergey Bravyi et al. *Tapering off qubits to simulate fermionic Hamiltonians*. 2017.

[3] Moran CC. *Mastering Quantum Computing with Ibm Qx*. Packt Publishing, 2019.

[4] Xie Chen. URL: https://www.its.caltech.edu/~xcchen/img/Ph223b2018/lecture/lecture0404.pdf.

[5] Xie Chen. URL: https://www.its.caltech.edu/~xcchen/img/Ph223b2018/lecture/lecture0402.pdf.

[6] Franck Laloë Claude Cohen-Tannoudji Bernard Diu. *Quantum Mechanics, Volume 3: Fermions, Bosons, Photons, Correlations, and Entanglement*. John Wiley Sons, 2019.

[7] Jeroen Dehaene and Bart De Moor. "Clifford group, stabilizer states, and linear and quadratic operations over GF(2)". In: *Physical Review A* (2003).

[8] Matthew P. A. Fisher et al. "Boson localization and the superfluid-insulator transition". In: *Phys. Rev. B* (1989).

[9] J. K. Freericks and H. Monien. "Phase diagram of the Bose-Hubbard Model". In: *Europhysics Letters* (1994).

[10] Vlad Gheorghiu. "Standard form of qudit stabilizer groups". In: *Physics Letters A* (2014).

[11] Daniel Gottesman. "Stabilizer codes and quantum error correction". PhD thesis. California Institute of Technology, 1997.

[12] Xin-Yu Huang et al. *Qubitization of Bosons*. 2022.

[13] Yan-Chao Li and Hai-Qing Lin. "Quantum coherence and quantum phase transitions". In: *Scientific Reports* (2016).

[14] Greiner M et al. "Quantum phase transition from a superfluid to a Mott insulator in a gas of ultracold atoms". In: *Nature* (2002).

[15] Daniele Malpetti. "Thermodynamics of strongly interacting bosons on a lattice". PhD thesis. Université de Lyon, 2016.

[16] Isaac L. Chuang Micheal A. Nielsen. *Quantum Computation and Quantum Information*. Cambridge University Press, 2010.

[17] Ryan V. Mishmash et al. "Hierarchical Clifford Transformations to Reduce Entanglement in Quantum Chemistry Wave Functions". In: *Journal of Chemical Theory and Computation* (2023).

[18] Bo Peng et al. *Quantum Simulation of Boson-Related Hamiltonians: Techniques, Effective Hamiltonian Construction, and Error Analysis*. 2023.

[19] Arthur Pesah. *A bird's-eye view of quantum error correction and fault tolerance*. URL: `https://arthurpesah.me/blog/2022-01-25-intro-qec-1/`.

[20] Arthur Pesah. *All you need to know about classical error correction*. URL: `https://arthurpesah.me/blog/2022-05-21-classical-error-correction/`.

[21] Arthur Pesah. *The stabilizer trilogy I — Stabilizer codes*. URL: `https://arthurpesah.me/blog/2023-01-31-stabilizer-formalism-1/`.

[22] Dario Picozzi and Jonathan Tennyson. "Symmetry-adapted encodings for qubit number reduction by point-group and other Boolean symmetries". In: *Quantum Science and Technology* (2023).

[23] Qiskit contributors. *Qiskit: An Open-source Framework for Quantum Computing*. 2023. DOI: `10.5281/zenodo.2573505`.

[24] *Qiskit Nature*. DOI: `https://doi.org/10.5281/zenodo.7828768`. URL: `https://github.com/qiskit-community/qiskit-nature%22`.

[25] Gabrielle Lya Castiaux Roberts. "Quantum fluids in a Bose-Hubbard circuit". PhD thesis. University of Chicago, 2023.

[26] Kanav Setia et al. "Reducing Qubit Requirements for Quantum Simulations Using Molecular Point Group Symmetries". In: *Journal of Chemical Theory and Computation* (2020).

[27] *Symmer*. URL: `https://github.com/UCL-CCS/symmer`.

[28] Francesco Terranova. *A Modern Primer in Particle and Nuclear Physics*. Oxford University Press, 2021.

[29] Yu Tong et al. "Provably accurate simulation of gauge theories and bosonic systems". In: *Quantum* (2022).

[30] Robin J. Wilson. *Introduction to Graph Theory*. Longman Group Ltd, 1996.

[31] Thomas G. Wong. *Introduction to Classical ad Quantum Computing*. Rooted Grove, 2022.